# Kendrick Mass Defect Spectrum: A Compact Visual Analysis for Ultrahigh-Resolution Broadband Mass Spectra

Christine A. Hughey,[†] Christopher L. Hendrickson, Ryan P. Rodgers, and Alan G. Marshall[†,*]

*Ion Cyclotron Resonance Program, National High Magnetic Field Laboratory, Florida State University,*
*1800 East Paul Dirac Drive, Tallahassee, Florida 32310*
Kuangnan Qian

*ExxonMobil Research and Engineering, 1545 Route 22 East, Annandale, New Jersey 08801*

At currently achievable Fourier transform ion cyclotron resonance broadband mass spectrometry resolving power ($m$/¢$m_{50\%}$ > 350 000 for 200 < $m/z$ < 1000), it would be necessary to spread out a conventional mass spectrum over ˘200 m in order to provide visual resolution of the most closely resolved peaks. Fortunately, there are natural gaps in a typical mass spectrum, spaced 1 Da apart, because virtually no commonly encountered elemental compositions yield masses at those values. Thus, it is possible to break a broadband mass spectrum into 1-Da segments, rotate each segment by 90 , scale each segment according to its mass defect (i.e., difference between exact and nominal mass), and then compress the spacing between the segments to yield a compact display. For hydrocarbon systems, conversion from IUPAC mass to "Kendrick" mass (i.e., multiplying each mass by 14.00000/14.01565) further simplifies the display by rectilinearizing the peak patterns. The resulting display preserves not only the "coarse" spacings (e.g., ˘1 Da between odd and even masses, corresponding to either even vs odd number of nitrogens or $^{12}C_c$ vs $^{12}C_{c-1}{}^{13}C_1$ elemental compositions of the same molecule; ˘2-Da separations, corresponding to a double bond or ring; ˘14 Da separations, corresponding to one CH$_2$ group) but also the "fine structure" (i.e., different mass defects for dif-ferent elemental compositions) across each 1-Da segment. The method is illustrated for experimental electrospray ionization FTICR ultrahigh-resolution mass spectra of a petroleum crude oil. Several thousand elemental compo-sitions may be resolved visually in a single one-page two-dimensional display, and various compound familiess class ($N_nO_oS_s$), type ($Z$ in $C_cH_{2c+Z}N_nO_oS_s$), and alkylation seriessmay be identified visually as well.

It is possible to generate molecular ions (M$^+$ from low-voltage electron impact (LVEI), field ionization/field desorption (FI/FD)) or quasimolecular ions (e.g., (M + H)$^+$, ( M - H)$^-$ by chemical ionization (CI), matrix-assisted laser desorption ionization (MAL-DI), electrospray ionization (ESI)), without significant fragmenta-tion. The advent of routine broadband ultrahigh-resolution Fourier transform ion cyclotron resonance mass spectrometry (FTICR MS)[1,2] makes it possible to resolve up to thousands of different elemental compositions (and thus thousands of chemically distinct components in the original sample) in a single mass spectrum.[3] In fact, viewed simply as a one-dimensional isocratic separation, FTICR MS offers up to 25 billion theoretical plates![4]

Fortunately, ultrahigh-resolution mass spectrometry offers much more than separation of chemically distinct constituents in a complex mixture such as petroleum crude oil. First, since each nuclide has a different mass defect (i.e., exact mass minus nearest-integer mass), each ion of different elemental composition has a different mass. Thus, for ions up to ˘400 Da (and up 1000 Da for families of structurally related ions), measurement of ion mass to within ˘1 ppm can often yield a unique elemental composition, $C_cH_hN_nO_oS_sP_p$, for the corresponding neutral.[5] In petroleum analysis, it is common to define a compound "class" as all of the elemental compositions with the same heteroatom content (e.g., $O_3S$ or NS).

Second, since each additional ring or double bond decreases the number of hydrogens by 2, it is possible to determine the compound "type" (i.e., number of rings plus double bonds) from the number of hydrogens relative to carbons. It is common to denote type as the value of $Z$ in the elemental composition expressed as, $C_cH_{2c+Z}N_nO_oS_sP_p$. For example, a carbazole mol-ecule, $C_{12}H_9N$, contains 3 rings and 6 double bonds, so that $2c + Z$ ) 9, and $Z$ ) - 15. Thus, an alkylated carbazole has elemental composition, $C_cH_{2c-15}N$, and the shorthand notation for its compound class and type is -15N.

---

[†] Department of Chemistry.

(1) Marshall, A. G.; Hendrickson, C. L.; Jackson, G. S. *Mass Spectrom. Rev.* **1998**, *17*, 1 -35.
(2) Marshall, A. G. *Int. J. Mass Spectrom.* **2000**, *200*, 331-336.
(3) Qian, K.; Rodgers, R. P.; Hendrickson, C. L.; Emmett, M. R.; Marshall, A. G. *48th Am. Soc. Mass Spectrom. Annual Conf. Mass Spectrom. Allied Top.*, Long Beach, CA, 2000; WOB3:00,
(4) Marshall, A. G.; Dorsey, J. G., unpublished results.
(5) Beynon, J. H.; Williams, A. E. *Mass and Abundance Tables for Use in Mass Spectrometry*; Elsevier: New York, 1963.

Third, the repeating mass ($CH_2$) for a hydrocarbon family is 14.015 65 Da.[6] Thus, it becomes possible to recognize a series of compounds of the same class and type, but different extent of alkylation, by finding a series of mass spectral peaks differing by 14.015 65 Da in mass. In this connection, it is particularly useful to rescale the mass spectrum from the usual IUPAC mass scale (based on the $^{12}C$ atomic mass as exactly 12 Da) to the "Kendrick" mass scale:[7]

$$\text{Kendrick mass} = \text{IUPAC mass} \times (14/14.01565) \quad (1)$$

The Kendrick scale effectively converts the mass of $CH_2$ from 14.015 65 to exactly 14.000 00. Thus, homologous series (namely, compounds with the same constitution of heteroatoms and number of rings plus double bonds, but different numbers of $CH_2$ groups) will have identical Kendrick mass defect:

$$\text{Kendrick mass defect} = (\text{nominal Kendrick mass} - \text{exact Kendrick mass}) \quad (2)$$

Finally, an even- (or odd-) electron ion of even (or odd) mass must contain an odd (or even) number of nitrogen atoms.[8] (MALDI and ESI typically generate even-electron ions.)

It is therefore clear that extraction of molecular class, type, and carbon distribution from a complex mixture depends on resolving and measuring mass (to within ~0.001 Da or less for ions of up to 1500 Da) over a wide mass range. At currently available FTICR mass resolving power ($m/\Delta m_{50\%} > 350\,000$ for $200 < m/z < 1000$, in which $\Delta m_{50\%}$ is mass spectral peak full width at half-maximum peak height), it would be necessary to spread out a conventional mass spectrum over ~200 m (e.g., 1 mm per 4 mDa, times 800 000 mDa) in order to provide visual resolution of the most closely spaced peaks! In this paper, we present a new, compact mass spectral display that allows for visual resolution of up to thousands of peaks in a broadband ultrahigh-resolution mass spectrum.

## EXPERIMENTAL METHODS

**Sample Preparation.** The present Chinese crude oil was provided by ExxonMobil Research & Engineering Co. (Annandale, NJ) and contains 6510 ppm of nitrogen and a total acid number (TAN) of 1.22. For sample preparation, 20 mg of the crude was first dissolved in 3 mL of toluene and then diluted with 17 mL of methanol to give a final volume of 20 mL. The final solution was spiked with 30% $NH_4OH$ to give a final base concentration of 0.05% (to facilitate deprotonation of the acids and neutral nitrogen compounds found in the crude). All solvents and reagents were obtained from Fisher Scientific Co.

**Electrospray Ionization High-Field FTICR Mass Spectrometry.** The crude oil was analyzed at the National High Magnetic Field Laboratory in Tallahassee, FL, with a home-built 9.4-T Fourier transform mass spectrometer.[9] Data were collected and processed by a modular ICR data acquisition system (MIDAS).[10] Ions were generated externally by a microelectrospray source[11] under negative-ion conditions, and samples were delivered by a syringe pump at a rate of 400 nL/min. In negative-ion mode,[12] acidic hydrocarbons are selectively ionized by ESI. Typical ESI conditions were as follows: needle voltage, 2.0 kV; tube lens, 370 V; and heated capillary current, 4 A. Ions were accumulated externally in a linear octopole ion trap for 20 s and then transferred through rf-only multipoles to a Penning trap.[13] Ions were excited by frequency sweep (72−641 kHz at 150 Hz/$\mu$s at an amplitude of 200 $V_{p-p}$ across a 10-cm-diameter open cylindrical cell). The time-domain ICR signal was sampled in direct mode at 1.28 Msample/s for 3.27 s to yield 4 Mword time-domain data. A total of 200 time-domain data sets were coadded, zero-filled once, Hanning apodized, and fast Fourier transformed with magnitude computation.

**Mass Calibration.** Mass spectra were initially frequency-to-$m/z$ internally calibrated[14,15] with respect to a G2421A electrospray "tuning mix" from Agilent (extending down to 734 Da) and stearic acid (283 Da, to span the low-mass end of the spectrum). Spectra were then converted to Kendrick mass and recalibrated with respect to the $-2O_2$ series, to give a mass error of <0.3 ppm across the whole mass range, 200−1000 Da.

**Assignment of Elemental Compositions.** The mass values for (singly charged) ions of 225−1000 Da and >0.2% relative abundance (corresponding to 3 standard deviations of the baseline noise) were imported into an Excel spreadsheet. Measured masses were converted from the IUPAC mass scale to the Kendrick mass scale[7] as described previously.[16] Even and odd nominal Kendrick masses were then sorted by an Excel macro, and the Kendrick mass defect was calculated. Even and odd nominal Kendrick masses then underwent a multiple sorting procedure[17] as follows. Homologous series were identified by Kendrick mass defect and molecular formulas assigned to lower molecular weight members based solely on mass measurement to ±1 ppm. Elemental compositions were assigned by use of a mass calculator program limited to molecular formulas consisting of up to 100 $^{12}C$ atoms; up to 2 $^{13}C$, up to 200 $^{1}H$, up to 5 $^{14}N$, up to 5 $^{16}O$, up to 5 $^{32}S$, and up to 1 $^{34}S$. If two (or more) elemental compositions were found within the mass tolerance of ±1 ppm, one formula could usually be confirmed/eliminated unequivocally by the presence/absence of the corresponding nuclide containing one $^{13}C$. Because members of a homologous series differ only by integer multiples of $CH_2$, assignment of a single member of such a series usually sufficed to identify all higher-mass members.

---

(6) Audi, G.; Wapstra, A. H. *Nucl. Phys. A* **1995**, *595*, 409−425.

(7) Kendrick, E. *Anal. Chem.* **1963**, *35*, 2146−2154.

(8) McLafferty, F. W.; Turecek, F. *Interpretation of Mass Spectra*; University Science Books: Sausalito, CA, 1993.

(9) Senko, M. W.; Hendrickson, C. L.; Pasa-Tolic, L.; Marto, J. A.; White, F. M.; Guan, S.; Marshall, A. G. *Rapid Commun. Mass Spectrom.* **1996**, *10*, 1824−1828.

(10) Senko, M. W.; Canterbury, J. D.; Guan, S.; Marshall, A. G. *Rapid Commun. Mass Spectrom.* **1996**, *10*, 1839−1844.

(11) Emmett, M. R.; White, F. M.; Hendrickson, C. L.; Shi, S. D.-H.; Marshall, A. G. *J. Am. Soc. Mass Spectrom.* **1998**, *9*, 333−340.

(12) Qian, K.; Robbins, W. K.; Hughey, C. A.; Cooper, H. J.; Rodgers, R. P.; Marshall, A. G. *Energy Fuels*, in press.

(13) Senko, M. W.; Hendrickson, C. L.; Emmett, M. R.; Shi, S. D.-H.; Marshall, A. G. *J. Am. Soc. Mass Spectrom.* **1997**, *8*, 970−976.

(14) Ledford, E. B., Jr.; Rempel, D. L.; Gross, M. L. *Anal. Chem.* **1984**, *56*, 2744−2748.

(15) Shi, S. D.-H.; Drader, J. J.; Freitas, M. A.; Hendrickson, C. L.; Marshall, A. G. *Int. J. Mass Spectrom.* **2000**, *195/196*, 591−598.

(16) Qian, K.; Rodgers, R. P.; Hendrickson, C. L.; Emmett, M. R.; Marshall, A. G. *Energy Fuels* **2001**, *15*, 492−498.

(17) Hsu, C. S.; Qian, K.; Chen, Y. C. *Anal. Chim. Acta* **1992**, *264*, 79−89.

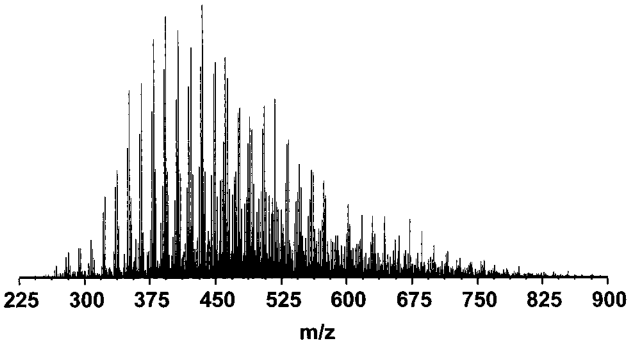

Figure 1. Broadband electrospray ionization FTICR mass spectrum of a heavy crude oil. The average resolving power across the spectrum is $m/\Delta m_{50\%}$ = 390 000 and the signal-to-noise ratio of the base peak is 1480:1.

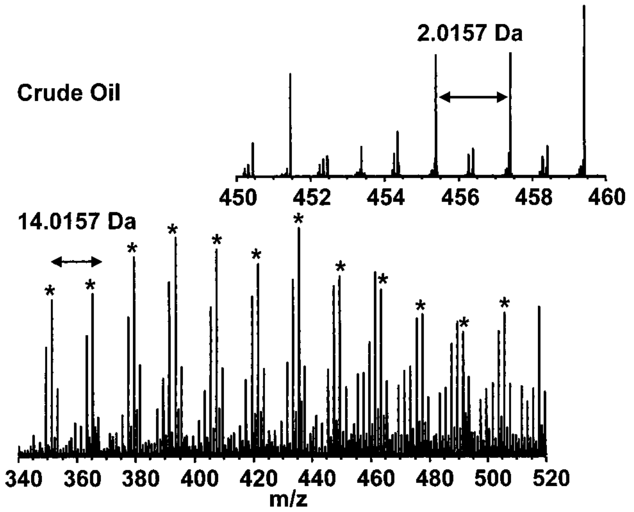

Figure 2. Mass scale-expanded segments of the full range petroleum mass spectrum of Figure 1. Species are present at every nominal mass, with obvious periodicities at every 2 (top) or 14 (bottom) nominal mass units.

## RESULTS AND DISCUSSION

**Conventional Ultrahigh-Resolution Mass Spectral Analysis.** A petroleum crude oil was chosen to illustrate the present approach. Although not as complex as a previously analyzed heavy petroleum crude oil[16] or asphaltene,[12] the present crude nevertheless yields an ESI FTICR negative-ion mass spectrum (see Figure 1) with thousands of resolved peaks of peak height above at least $3\sigma$ (as stated in the Experimental Section) of baseline noise. Figure 2 shows two successive mass scale expansions, revealing periodicities of ~14 (from compound series differing in number of $CH_2$ groups) and ~2 Da (from compound series differing in number of rings plus double bonds). Moreover, there is a clear alternation in ion relative abundance for even- versus odd-mass ions. The even-mass ions contain an odd number of nitrogens (typically one—see below), and the odd-mass ions contain zero or an even number of nitrogens (typically zero—see below).

Additional interpretation requires mass scale expansion to resolve different elemental compositions at a given nominal mass, as shown for ions of ~457 Da in Figure 3 (in IUPAC mass). The mass accuracy available from FTICR MS makes possible unique assignment of elemental compositions for all of the 15 resolved mass spectral peaks (see Table 1). Those elemental compositions in turn reveal the compound class and type. A similar display for an even nominal mass (not shown) reveals $^{12}C_{c-1}$ $^{13}C_1$ species corresponding to the same class and type $^{12}C_c$ (even-mass) compound, but higher in mass by 1.003 35 Da.[6]

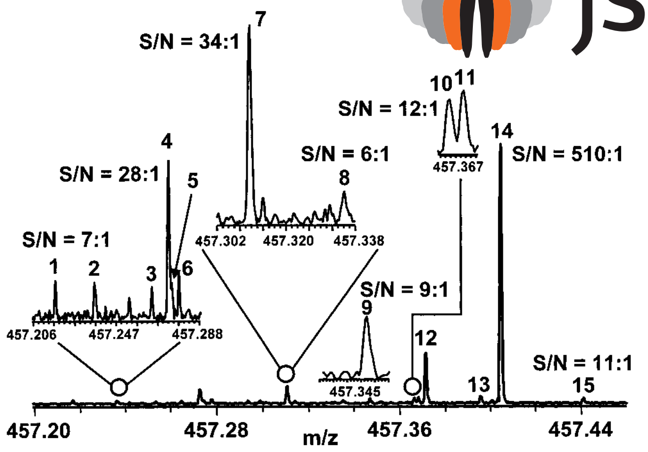

Figure 3. A further mass scale-expanded segment (plotted as IUPAC mass) of the crude oil mass spectrum of Figure 1, allowing for visual resolution and elemental composition assignment (based on accurate mass measurement) of all of the 15 chemically distinct species at a single nominal mass. The tabulated data for the 15 peaks show an average mass error of ~0.0001 Da for the proposed assignments. The elemental composition reveals both the "class" (i.e., number(s) of various heteroatoms) and "type" (i.e., number of rings plus double bonds), expressed according to the "$Z$" value in the chemical formula, $C_cH_{2c+Z}N_nO_oS_s$.

Identification of a series of compounds of the same class and type but different number of $CH_2$ groups is greatly facilitated by conversion to Kendrick mass, as seen from the data in Table 2. The series of masses differing in exact mass by 14.015 65 Da now becomes a series of mass differing by 14.000 00 Kendrick mass units. Stated another way, each member of such a series has the same "extension number" (i.e., the same three to four digits following the decimal point in Kendrick mass).

**Mass Defect Spectrum for Visual Analysis of Ultrahigh-Resolution Data.** Two features of an ultrahigh-resolution mass spectrum make possible a much more compact display of the data. First, as seen in broadband display in Figure 2 (top) and with $m/z$ scale expansion in Figure 3, the masses corresponding to chemically possible elemental compositions are not randomly distributed. Typical organic molecular formulas correspond to an approximately Gaussian distribution (e.g., ~0.5 Da width at ~600 Da), with near-zero abundance at 1-Da intervals. Second, the elemental composition information is contained within each ~0.5-Da-wide segment, whereas the remaining spectral features are spaced at intervals of 1−14 Da in nominal mass. Therefore, an ultrahigh-resolution mass spectrum offers a natural two-dimen-sional display, if the spectrum is sliced into 1-Da-wide segments and those segments are then stacked next to each other, as shown in the three-dimensional representation of Figure 4. The $x$-axis is nominal mass, the $y$-axis is mass defect, and the $z$-axis is the mass spectral signal magnitude. The nominal mass scale may then be compressed, thereby greatly increasing the number of peaks that may be seen in a single display.

As for most three-dimensional displays, it is helpful to project the data onto a two-dimensional surface, as in the two-dimensional contour plot spanning a nominal mass range of 200 Da shown for odd-mass ions in Figure 5. To avoid undue complexity, only a

Table 1. Elemental Composition Assignments for the 15 Resolved Peaks of Nominal Mass, 457 (Figure 3)[a]

| peak no. | measd mass | rel abund (%) | theor mass | error (mDa) | $m/\Delta m_{50\%}$ | type ($Z$) | class (NOS) |
|---|---|---|---|---|---|---|---|
| 1 | 457.2174 | 0.50 | 457.2173 | +0.1 | 517 000 | −36 | $O_2$ |
| 2 | 457.2367 | 0.47 | 457.2366 | +0.1 | 345 000 | −35 | $NO^{13}C$ |
| 3 | 457.2650 | 0.42 | 457.2649 | +0.1 | 413 500 | −32 | $N_2$ |
| 4 | 457.2731 | 2.01 | 457.2730 | +0.1 | 413 500 | −33 | $N^{13}C$ |
| 5 | 457.2747 | 0.47 | 457.2748 | −0.1 | 138 000 | −24 | $O_3$ |
| 6 | 457.2784 | 0.60 | 457.2782 | +0.2 | 413 500 | −14 | $O_3S$ |
| 7 | 457.3112 | 2.40 | 457.3112 | 0.0 | 413 500 | −22 | $O_2$ |
| 8 | 457.3357 | 0.40 | 457.3357 | 0.0 | 258 000 | −2 | $O_4S$ |
| 9 | 457.3475 | 0.64 | 457.3476 | −0.1 | 413 500 | −20 | O |
| 10 | 457.3669 | 0.74 | 457.3669 | 0.0 | 413 500 | −19 | $N^{13}C$ |
| 11 | 457.3687 | 0.85 | 457.3687 | 0.0 | 413 500 | −10 | $O_3$ |
| 12 | 457.3720 | 7.13 | 457.3721 | −0.1 | 413 500 | 0 | $O_3S$ |
| 13 | 457.3961 | 1.04 | 457.3961 | 0.0 | 413 500 | −10 | $O_2{}^{13}C_2$ |
| 14 | 457.4049 | 36.7 | 457.4051 | −0.2 | 517 000 | −8 | $O_2$ |
| 15 | 457.4416 | 0.74 | 457.4415 | +0.1 | 344 500 | −6 | O |

[a] The "Z" value in the chemical formula, $C_cH_{2c+Z}N_nO_oS_s$, is related to the number of rings plus double bonds. Note that the listed masses refer to the observed (deprotonated) species but that the "Z" values are calculated for the corresponding neutral.

Table 2. Kendrick Masses for Crude Oil *Z*-Series, $-2O_2$

| measd mass (Da) | rel abund (%) | Kendrick mass | theor Kendrick mass | error (mDa) | Kendrick mass defect | molecular formula $[M - H]^-$ |
|---|---|---|---|---|---|---|
| 351.3269 | 69.12 | 350.9346 | 350.9346 | 0.0 | 0.066 | $C_{23}H_{43}O_2$ |
| 365.3425 | 71.28 | 364.9346 | 364.9346 | 0.0 | 0.066 | $C_{24}H_{45}O_2$ |
| 379.3581 | 88.50 | 378.9346 | 378.9346 | 0.0 | 0.066 | $C_{25}H_{47}O_2$ |
| 393.3738 | 95.89 | 392.9346 | 392.9346 | 0.0 | 0.066 | $C_{26}H_{49}O_2$ |
| 407.3894 | 91.48 | 406.9346 | 406.9346 | 0.0 | 0.066 | $C_{27}H_{51}O_2$ |
| 421.4051 | 84.40 | 420.9346 | 420.9346 | 0.0 | 0.066 | $C_{28}H_{53}O_2$ |
| 435.4207 | 100.00 | 434.9346 | 434.9346 | 0.0 | 0.066 | $C_{29}H_{55}O_2$ |
| 449.4364 | 80.72 | 448.9346 | 448.9346 | 0.0 | 0.066 | $C_{30}H_{57}O_2$ |
| 463.4519 | 75.09 | 462.9344 | 462.9346 | −0.2 | 0.066 | $C_{31}H_{59}O_2$ |
| 477.4676 | 62.50 | 476.9345 | 476.9346 | −0.1 | 0.066 | $C_{32}H_{61}O_2$ |
| 491.4831 | 54.80 | 490.9344 | 490.9346 | −0.2 | 0.066 | $C_{33}H_{63}O_2$ |
| 505.4989 | 64.56 | 504.9345 | 504.9346 | −0.1 | 0.066 | $C_{34}H_{65}O_2$ |

single contour is shown (namely, peaks with magnitude greater than 3$\sigma$ of baseline noise). Two patterns in Figure 5 have immediate chemical relevance. First, many data points clearly fall on several slanted parallel lines (e.g., dashed line in Figure 5), in which successive peaks are separated by 14 Da in nominal mass (and 0.015 65 Da in mass defect), corresponding to compounds of the same class and type but different number of $CH_2$ groups. Second, other sets of parallel lines of data result from successive peaks separated by 2 Da in nominal mass and 0.015 65 Da in mass defect, corresponding to compounds of the same class but different type (i.e., different number of rings plus double bonds).

**Analogy to Echelle Optics.** It is worth noting that high-resolution optical spectroscopy (notably atomic emission from an inductively coupled plasma) affords a close parallel to the present mass spectral analysis. An optical emission spectrum from a sample containing many elements may present hundreds to thousands of lines, whose linear resolution would require an inconveniently long spatial dimension for electronic detection. The most compact optical detectors are rectilinear arrays, such as charge-coupled devices (CCDs). Thus, optical emission is efficiently detected by directing the spectral range of interest from an "echelle" grating.[18] The grating is steeply ruled, to generate multiple overlapped diffraction orders. Passage of the echelle-diffracted light through a prism allows for focusing of the output onto a CCD array detector in such a way that a spectral segment from one diffraction order is displaced vertically from an adjoining spectral segment from the next diffraction order. (In practice, the segments are design to overlap slightly, to avoid losing any

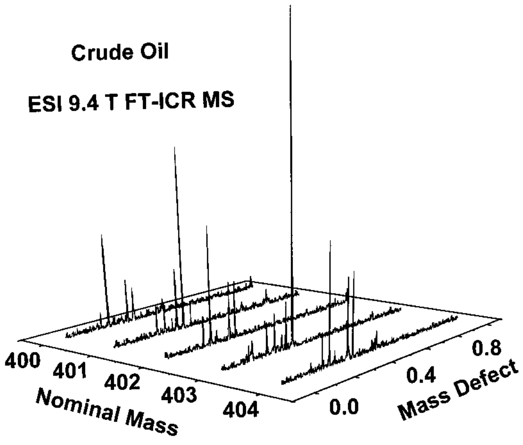

Figure 4. Three-dimensional display of a 5-Da segment of the mass spectrum of Figure 1. The spectrum has been sliced into 1-Da segments, and each segment is then rotated by 90° and scaled according to its "mass defect" (i.e., difference between exact and nominal mass). The segments are then stacked according to their nominal mass as shown.

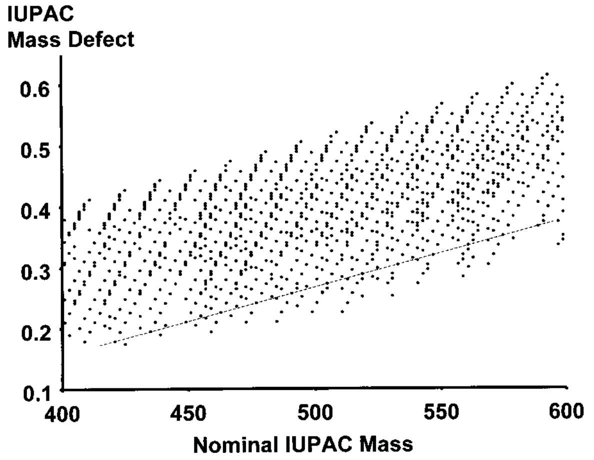

Figure 5. Plot of IUPAC mass defect vs nominal IUPAC mass for ions of *odd* nominal mass within a 200-Da segment of the mass spectrum of Figure 1. (It is convenient to display the even-mass and odd-mass data separately.) Note the periodicities of 2 and 14 Da on the nominal mass axis, as well as 0.015 65 Da (i.e., mass defect for two hydrogens) on the mass defect axis. These spacings make it possible to determine molecular "class" and "type" simultaneously over a wide mass range from a single display (see Figure 6 ff).

spectral elements at the "joints" between successive segments.) The net result is to cut the original spectrum into segments, and stack them on top of each other, to give a final result highly similar to the mass defect versus nominal mass plot of Figure 5 for mass spectral data.

**Kendrick Mass.** An obvious complication of the two-dimensional mass spectral display of Figure 5 is the skewing of the data to fall on slanted lines. The reason is that a nominal mass difference of 2 (corresponding to $H_2$) or 14 (corresponding to $CH_2$) on the horizontal axis is accompanied by simultaneous shift in mass defect by 0.015 65 Da on the vertical axis (hence, lines of finite slope for series of compounds differing in either number of $CH_2$ groups or number of rings plus double bonds). However, if one rescales the data from IUPAC mass to Kendrick mass, the nominal mass differences will be the same, but the mass defects for a series of compounds differing by multiples of $CH_2$ will now differ by $14.01565(14.00000/14.01565) - 14 = 0$, rather than 0.015 65 Da, as seen for even-mass $^{12}C_c$ ions in Figure 6. Compounds of the same class and type but different number of $CH_2$ units will thus fall on a single horizontal line, with peaks separated by 14 Da in nominal mass but zero difference in Kendrick mass defect. Similarly, compounds of the same class but different type (i.e., differing by $H_2$) will fall on horizontal lines separated by $2.01565(14.00000/14.01565) - 2.00000 = 0.013\,40$ difference in Kendrick mass defect. Compounds of different class are now readily identified, because the Kendrick mass defect for compounds of a given class will be displaced vertically from those of other classes (note the vertical separation between the N, NO, and $NO_2$ classes in Figure 6). Finally, if an elemental composition for a compound whose carbons are all $^{12}C$ is assigned at a given *even* mass, then one would expect to find the same elemental composition, except with one $^{13}C$ instead of $^{12}C$, at an *odd* mass, 1.003 35 Da (IUPAC) mass units higher than the corresponding even-mass peak. It is satisfying to note that the data for compounds containing one $^{13}C$ (Figure 7) nicely corroborate several of the assignments in Figure 6. Note that a number of types of the $O_2{}^{13}C_2$ class are identified as well.

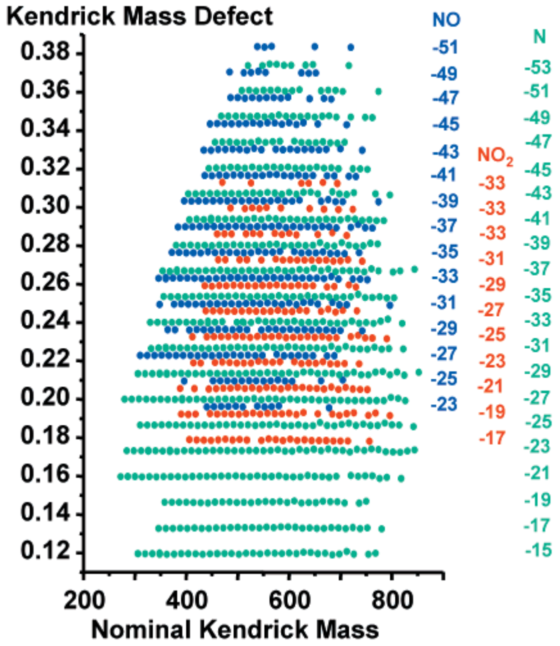

Figure 6. Kendrick mass defect vs nominal Kendrick mass (full mass range) for *even*-mass $^{12}C_c$ ions. The replacement of IUPAC mass by Kendrick mass converts the skewed display (e.g., Figure 5) into a rectilinear display, for simpler visual interpretation. Note the visual *vertical* separation of compound classes (e.g., N vs NO) and types (compounds with different number of rings plus double bonds) based on mass defect and the simultaneous visual *horizontal* distribution of number of $CH_2$ groups for a given compound class and type.

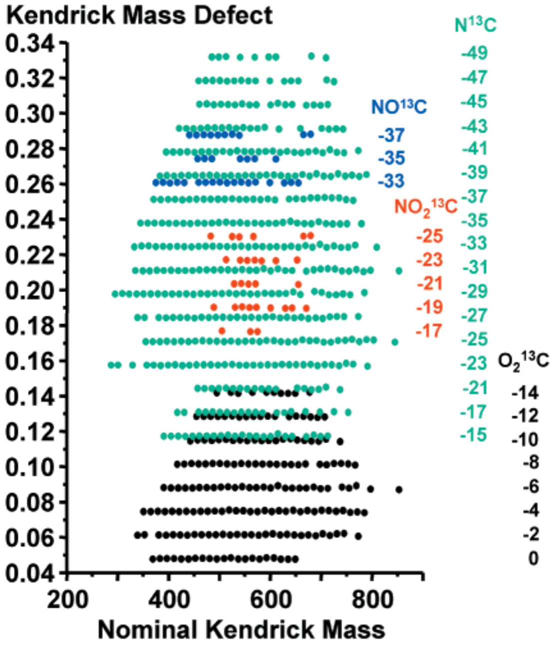

Figure 7. Kendrick mass defect vs nominal Kendrick mass (full mass range) for *odd*-mass $^{12}C_{c-1}{}^{13}C$ ions corresponding to the *even*-mass $^{12}C_c$ ions of Figure 6. The observation of each $^{12}C_{c-1}{}^{13}C$ series at *odd* mass corroborates the assignment of the corresponding $^{12}C_c$ species at *even* mass.

---

(18) Busch, K. W.; Busch, M. A. In *Multielement Detection Systems for Spectrochemical Analysis*; Busch, K. W., Busch, M. A., Eds.; Wiley-Interscience: New York, 1990; Vol. 107, pp 125−129.

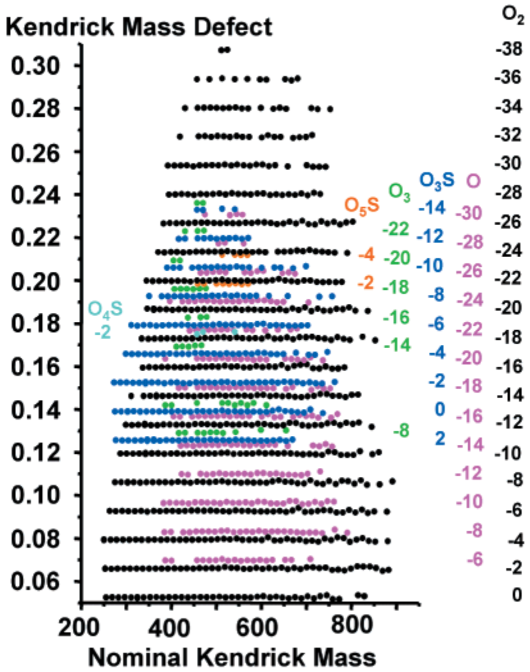

Figure 8. Kendrick mass defect vs nominal Kendrick mass for *odd*-mass $^{12}C_c$ ions. Note the visual *vertical* separation of compound classes (O, $O_2$, $O_3S$) and types (e.g., compounds with different number of rings plus double bonds) based on mass defect and the simultaneous visual *horizontal* distribution of number of $CH_2$ groups for a given compound class and type.

Similar plots of Kendrick mass defect versus nominal Kendrick mass are shown for $^{12}C_c$ ions of *odd* nominal mass in Figure 8 and their corresponding $^{13}C^{12}C_{c-1}$ isotopic variants at *even* nominal mass (not shown). Six distinct $^{12}C_c$ classes at odd masses are resolved in Figure 8: O, $O_2$, $O_3$, $O_3S$, $O_4S$, and $O_5S$. Three of those class assignments are confirmed by observation of their $^{13}C^{12}C_{c-1}$ isotopic variants, and in addition, a type series of the $N^{13}C_2$ class is seen.

Graphical display of such data offers other advantages. First, "outlier" data are more readily recognized if they fall outside the main patterns. Second, once a series of related compounds has been identified, then extension of that pattern to higher mass allows for convincing elemental composition assignment of ions whose mass would otherwise be too high to allow for unique assignment based only on the measured mass of that peak. Thus, despite increasing vertical uncertainty with increasing nominal mass in the plots of Figures 6−8, it is still possible to assign the high-mass peaks with confidence by extrapolation from lower-mass members of an existing carbon series.

Figure 9 presents a two-dimensional display of Kendrick mass defect versus nominal Kendrick mass, for *all* mass spectral peaks higher than $3\sigma$ of baseline noise, including ions of even and odd mass as well as species containing one or two $^{13}C$ atoms. Some 3900 peaks are present in this single one-page display, and the various classes, types, and carbon distributions may be determined from the various patterns described in Figures 6−8.

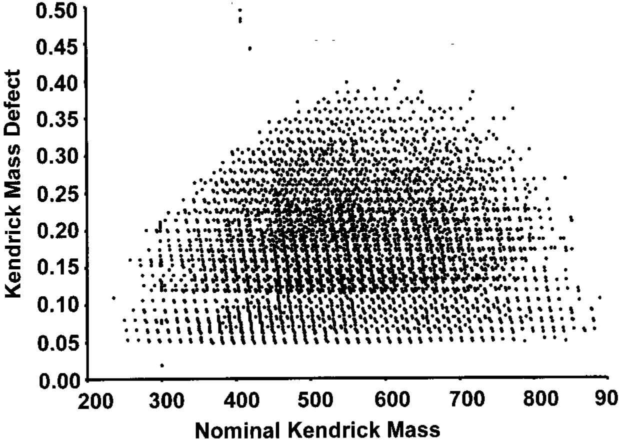

Figure 9. Kendrick mass defect vs nominal Kendrick mass for *all* resolved peaks in the broadband ESI FTICR negative-ion mass spectrum of Figure 1. This single-page display not only visually resolves virtually all of the 3900 (!) peaks in the original mass spectrum but also reveals each ion's class and type (by projection to the vertical axis), and carbon distribution (by projection to the horizontal axis).

In the present examples, all ions are singly charged. However, the present mass defect display can be adapted to multiply charged ions. Because FTICR mass resolving power makes it easy to determine the charge state (from the reciprocal of the $m/z$ spacing between the $^{12}C_n$ and $^{13}C_1{}^{12}C_{n-1}$ signals from a given ion)[19−21] one can simply convert from $m/z$ to mass scale and then proceed as in this paper.

---

(19) Senko, M. W.; Beu, S. C.; McLafferty, F. W. *J. Am. Soc. Mass Spectrom.* **1995**, *6*, 52−56.

(20) Zhang, Z.; Marshall, A. G. *J. Am. Soc. Mass Spectrom.* **1998**, *9*, 225−233.

(21) Horn, D. M.; Zubarev, R. A.; McLafferty, F. W. *J. Am. Soc. Mass Spectrom.* **2000**, *11*, 320−332.

## CONCLUSION

We propose that the present two-dimensional display of Kendrick mass defect versus nominal Kendrick mass be adopted as a standard means for visualizing (and assigning) elemental composition patterns in ultrahigh-resolution mass spectra of complex organic mixtures. This approach offers the advantage of compact display similar to that of echelle optics for array detection of optical spectra, with additional advantages of visual resolution and identification of compound classes, types, and carbon distributions. Compared to conventional tabulation of data, in which only one or a few compound series can be considered at a time, the two-dimensional display allows for simultaneous examination of several (or even all) classes, types, and carbon distributions at once. Also, the graphical approach simplifies the identification of spurious peaks. Finally, graphical display makes it easier to recognize higher-mass members of a given compound series and thus facilitates elemental composition assignment at high mass.

## ACKNOWLEDGMENT

This work was supported by the NSF National High-Field FT-ICR Mass Spectrometry Facility (CHE 99-09502), Florida State University, and the National High Magnetic Field Laboratory at Tallahassee, FL. The authors thank ExxonMobil for their support of the exploratory research and for permission to publish the data.

Received for review May 17, 2001. Accepted July 25, 2001.

AC010560W